# Protein Folding Triggered by Electron Transfer

Torbjörn Pascher, John P. Chesick, Jay R. Winkler,* Harry B. Gray*

Rapid photochemical electron injection into unfolded ferricytochrome *c* titrated with 2.3 to 4.6 M guanidine hydrochloride (GuHCl) at pH 7 and 40°C produced unfolded ferrocytochrome, which then converted to the folded protein. Two folding phases were observed: a fast process with a time constant of 40 microseconds (4.6 M GuHCl), and a slower phase with a rate constant of 90 ± 20 per second (2.3 M GuHCl). The activation free energy for the slow step varied linearly with GuHCl concentration; the rate constant, extrapolated to aqueous solution, was 7600 per second. Electron-transfer methods can bridge the nanosecond to millisecond measurement time gap for protein folding.

Understanding how the secondary and tertiary structures of proteins are formed from nonnative conformations is a continuing challenge for theory (*1*, *2*) and experiment (*3*–*8*). The essential requirement for experimental investigations of protein-folding kinetics is some means of triggering the folding (or unfolding) process. A common technique involves rapid dilution, usually by stopped-flow mixing, of a solution containing protein and a denaturant. The lowered denaturant concentration in the mixed solution shifts the equilibrium toward the folded protein structure. The "dead time" in these experiments, typically a few milliseconds or more, is too long to permit studies of the collapse to a compact denatured state (the burst phase) in many protein-folding reactions (*7*). Triggering methods that allow measurements on faster time scales are needed to uncover the earliest events in protein folding (*9*).

Thermodynamic analyses suggest that many redox-active proteins will be amenable to a protein-folding trigger based on electron-transfer (ET) chemistry. A simple cycle can be drawn connecting an oxidized ($P_{OX}$) and reduced ($P_{RED}$) protein in both folded (F) and unfolded (U) configurations (Fig. 1) (*10*). If the active site reduction potentials for the folded and unfolded states, $E_F$ and $E_U$, are different ($\Delta E_f \equiv E_F - E_U$), then the free energies of folding the oxidized and reduced proteins, $\Delta G_{f,OX}$ and $\Delta G_{f,RED}$, will differ by a comparable amount ($\Delta\Delta G_f \equiv \Delta G_{f,OX} - \Delta G_{f,RED}$). If $\Delta\Delta G_f$ is sufficiently large, denaturing conditions can be found in which one oxidation state of the protein is fully unfolded whereas the other is fully folded. A rapid ET reaction can then initiate a folding (or unfolding) process. It is important that the redox-active cofactor remains bound to the unfolded protein so that the rate-determining step is folding rather than a bimolecular cofactor-capture process. In proteins where $\Delta E_f$ is not large, it may be possible to modify the active site reduction potential by means of site-directed mutagenesis. ET-initiated folding, which can be applied to any redox-active protein with a reduction potential that differs sufficiently from that of the cofactor in aqueous solution, has great promise because of the many well-established techniques for rapidly injecting and removing electrons from proteins on time scales as short as a few nanoseconds.

We used a heme protein, cytochrome *c*, to evaluate this approach. The reduction potential of the unfolded protein can be approximated by that of an exposed heme in aqueous solution [$E_U \approx -100$ to $-200$ mV versus the normal hydrogen electrode (NHE) (*10*, *11*)]. The heme potential in folded cytochrome *c* is substantially greater [$E_F = 260$ mV versus NHE (*12*)]. This marked increase in potential upon protein folding indicates that reduced cytochrome *c* (cyt $c^{II}$) is more stable toward unfolding than is the oxidized protein (cyt $c^{III}$). Titrations of cyt $c^{II}$ and cyt $c^{III}$ with guanidine hydrochloride (GuHCl) at pH 7 and 40°C (probed by Trp fluorescence) clearly illustrate this point (Fig. 2) (*3*, *13*). The folding free energies for oxidized and reduced proteins depend linearly on [GuHCl] (Fig. 2B), and extrapolating to [GuHCl] = 0 gives values for the free energy of folding in aqueous solution (cyt $c^{II}$, $-\Delta G^{\circ}_{f,RED} = 61 \pm 10$ kJ mol$^{-1}$; cyt $c^{III}$, $-\Delta G^{\circ}_{f,OX} = 30 \pm 1$ kJ mol$^{-1}$). These extrapolated values are consistent with the difference in reduction potentials of the folded and unfolded proteins.

Rapid reduction of unfolded ferricytochrome (cyt $c^{III}_U$) in the range of 2.3 to 5.0 M GuHCl will produce unfolded ferrocytochrome (cyt $c^{II}_U$), which must then undergo a conformational change to its equilibrium folded state (cyt $c^{II}_F$). In initial experiments, Ru(2,2′-bipyridine)$_3^{2+}$ ($Ru^{2+}$) was used as a photosensitizer to inject electrons into cyt $c^{III}_U$ (Fig. 3). Visible excitation of this complex generates a long-lived excited state ($*Ru^{2+}$, exponential decay time $\tau \approx 0.6$ μs) that is capable of reducing cyt $c^{III}_U$ to the ferrous state [$E^{\circ}(Ru^{3+}/*Ru^{2+}) = -0.84$ V versus NHE] (*14*). The power of this approach is that, with pulsed-laser excitation (480 nm, 20 ns), cyt $c^{II}_U$ is formed in <1 μs, thus permitting the observation of early folding events (*15*). The reoxidation of cyt $c^{II}$ by $Ru^{3+}$ ($k_r$, Fig. 3) limits measurements to times shorter than ~1 ms. After injecting electrons from $*Ru^{2+}$ into cyt $c^{III}_U$ at 4.6 M GuHCl, we observed rapid changes in the visible absorption spectrum that are consistent with a cyt $c^{II}$ folding process. The time constant for formation of this folding intermediate (cyt $c^{II}_I$) is ~40 μs at pH 7 and 40°C. This observation is consistent with studies of cyt $c^{II}$ folding after CO dissociation (*3*). A plausible interpretation of this result is that this phase corresponds to the collapse of the unfolded protein into a compact de-

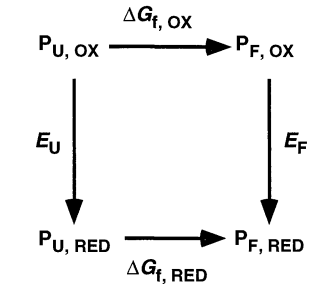


**Fig. 1.** Thermodynamic cycle illustrating the relation between folding free energies ($\Delta G_f$) and reduction potentials ($E$) for the unfolded (U) and folded (F) states of oxidized ($P_{OX}$) and reduced ($P_{RED}$) proteins.

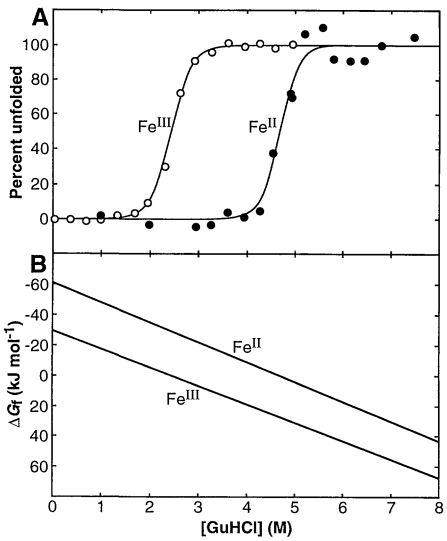


**Fig. 2.** (**A**) Folding titration curves for oxidized ($Fe^{III}$) and reduced ($Fe^{II}$) cytochrome *c*, obtained with the use of GuHCl as a denaturant (pH 7 and 40°C). (**B**) Dependence of folding free energies on [GuHCl] for oxidized and reduced cytochrome *c* (pH 7 and 40°C).

T. Pascher, J. R. Winkler, H. B. Gray, Beckman Institute 139-74, California Institute of Technology, Pasadena, CA 91125, USA.
J. P. Chesick, Haverford College, Haverford, PA 19041, USA.
*To whom correspondence should be addressed.

natured structure. A similar explanation has been offered for the fast-folding kinetics of cold-denatured barstar (*9*) and apomyoglobin (*16*).

Further changes in optical absorption spectra are expected to occur in cyt $c^{II}$ folding during the rearrangement of the peptide around the heme to yield the native protein configuration. To probe this slower phase of cyt $c^{II}$ folding, we used an electron-injection system based on $Co(ox)_3^{3-}$ (ox, $C_2O_4^{2-}$) photochemistry. Photolysis of $Co(ox)_3^{3-}$ with a 308- or 266-nm laser pulse generates a reducing species, presumably the carbon dioxide radical anion ($CO_2^{\cdot-}$), that rapidly (<1.0 ms) injects an electron into cyt $c_U^{III}$ (Fig. 3). At >4 M GuHCl, the observed kinetics are dominated by the oxidation of cyt $c_I^{II}$ to cyt $c_U^{III}$ by $Co(ox)_3^{3-}$ and traces of $O_2$ ($k_o$, Fig. 3). The folding rate constant ($k_{f2}$, Fig. 3) increases with decreasing [GuHCl], and for ≤3.5 M GuHCl, the reoxidation process is slower than folding. At 2.3 to 3.5 M GuHCl (pH 7 and 40°C), clear spectroscopic evidence is obtained for the formation of fully folded cyt $c^{II}$ (Fig. 4). Multipoint transient absorption spectra agree well with difference spectra obtained from oxidized and reduced cyt *c* in solutions of high and low denaturant concentrations.

The long time-scale (>1 ms) folding kinetics measured in the region of the heme Soret absorption (400 and 420 nm) can be described by a sum of two exponentials. The slower rate (~1 $s^{-1}$), which was not determined precisely at 40°C in our experiments, is attributable to oxidation of cyt $c_F^{II}$ by $Co(ox)_3^{3-}$ or to a slower folding process. The faster rate corresponds to the bulk of the measured absorbance change and was found to be independent of eightfold variations in the concentrations of cyt *c*. On the basis of the steady-state spectra of folded and unfolded cyt $c^{II}$, the observed rate constant for this process can be decomposed into a sum of the cyt $c_I^{II}$ folding rate ($k_{f2}$) and the rate for cyt $c_I^{II}$ oxidation ($k_o = 11 \pm 5$ $s^{-1}$) (*17*). The data suggest that the final step in the formation of cyt $c_F^{II}$ is a simple first-order process, and, unlike ferricytochrome folding (*4*, *5*), the kinetics do not appear to be heterogeneous. In fact, the kinetics of the final cyt $c^{II}$ folding step resemble those of cyt $c_U^{III}$ at pH < 5, where nonnative His ligation to the heme is inhibited. One possible explanation is that the cyt $c_U^{II}$ heme undergoes faster axial-ligand exchange than does the ferriheme, such that interconversions among incorrectly ligated hemes may not be rate-limiting in the folding reaction (*18*).

The measured rate constants for the conversion of cyt $c_I^{II}$ to cyt $c_F^{II}$ are a sensitive function of [GuHCl]; $k_{f2}$ decreases from 90 ± 20 $s^{-1}$ at 2.3 M GuHCl to 15 ± 5 $s^{-1}$ at 3.2 M GuHCl. A plot of ln $k_{f2}$ versus [GuHCl] (2.3 to 3.9 M, pH 7, 40°C) is linear (Fig. 5) (*19*). Because the free energy of cyt $c_U^{II}$ folding ($-\Delta G_f$) also varies linearly with [GuHCl] (Fig. 2), we can infer that ln $k_{f2}$ is a linear function of the folding driving force. This behavior is consistent with that found for T4 lysozyme folding, where both the protein folding and unfolding rate constants exhibit linear free-energy dependences (*20*). An analysis of this behavior in terms of protein solvation in mixed solvents suggests that the [GuHCl] dependence of $k_{f2}$ can be described by

$$\ln k_{f2} = \ln k_{f2}^{o} - \Delta\beta_2^{o\ddagger}[\text{GuHCl}] \quad (1)$$

where $\Delta\beta_2^{o\ddagger}$ is the free energy of transfer of the transition state from aqueous solution to denaturant solution per unit of molarity, and $k_{f2}^{o}$ is the folding rate constant in the absence of GuHCl (*20*). A fit of the cyt $c^{II}$ folding data to Eq. 1 yields $k_{f2}^{o} = 7.6 \times 10^3$ $s^{-1}$ and $\Delta\beta_2^{o\ddagger} = 1.9$ $M^{-1}$.

Although there have been few investigations of cyt $c^{II}$ folding (*3*, *21*, *22*), the oxidized protein has been studied in great detail (*3–5*, *23*, *24*). Extrapolation of cyt $c^{II}$ kinetics data to a denaturant concentration of 0.7 M (typical of work with cyt $c^{III}$) yields an estimated folding rate constant of $2.0 \times 10^3$ $s^{-1}$ (at pH 7 and 40°C) for the reduced protein. Temperature extrapolations are far more tenuous, but, assuming an estimated activation enthalpy of 30 kJ $mol^{-1}$, we predict $k_{f2} = 530$ $s^{-1}$ at 10°C for cyt $c^{II}$ (*25*). This value may be compared to the rate of 68 $s^{-1}$ (0.7 M GuHCl, pH 6.9, 10°C) reported for cyt $c^{III}$ folding (*4*, *26*). It is also possible to compare folding rates at a constant free-energy change. At 0.7 M GuHCl and 10°C, cyt $c^{III}$ folding has a free-energy change comparable with that for cyt $c^{II}$ folding at 2.2 M GuHCl and 40°C, and the corresponding folding rate constants are 68 $s^{-1}$ (cyt $c^{III}$) and 115 $s^{-1}$ (cyt $c^{II}$).

Redox thermodynamic considerations indicate that the folding energetics for cyt $c^{II}$ are quite distinct from those for cyt $c^{III}$. The entropy change for reduction of folded cyt $c^{III}$ ($\Delta S_{RC}$) is $-62 \pm 5$ J $mol^{-1}$ $K^{-1}$ (*12*, *27*). The temperature dependence of the reduction potential of unfolded cyt *c* has not been measured, but a value of $\Delta S_{RC} = 12.5$ J $mol^{-1}$ $K^{-1}$ has been reported for Fe(1,10-phenanthroline)$_3^{3+/2+}$ (*28*). An entropy cycle analogous to the free-energy cycle in Fig. 1 indicates that the entropy change for folding cyt $c^{II}$ is roughly 60 J $mol^{-1}$ $K^{-1}$ more negative than that for cyt $c^{III}$. The folding entropy of cyt $c^{II}$ is offset by a highly favorable enthalpy of folding, at least 50 kJ $mol^{-1}$ greater than that for cyt

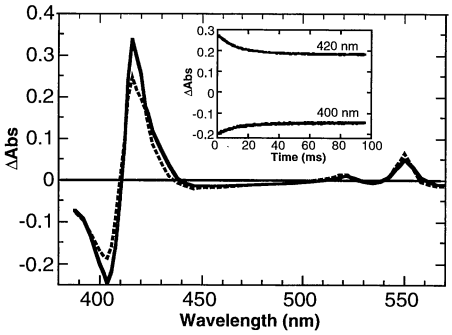


**Fig. 4.** Transient difference spectra recorded after electron injection into cyt $c_U^{III}$ (2.7 M GuHCl, pH 7, 40°C). ΔAbs is the difference in absorption between the transient species and cyt $c_U^{III}$. The curves are [cyt $c_I^{II}$–cyt $c_U^{III}$] (solid line, recorded immediately) and [cyt $c_F^{II}$–cyt $c_U^{III}$] (dashed line, recorded after 50 ms) difference spectra. The inset shows the kinetics recorded at two wavelengths in the Soret region.

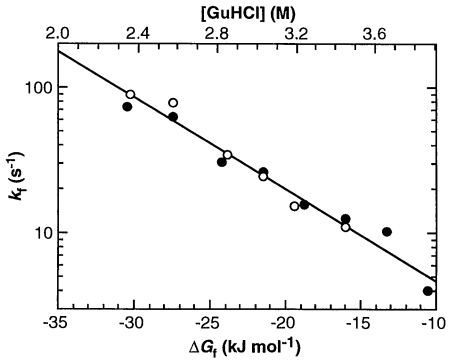


**Fig. 5.** Variation of cyt $c^{II}$ folding rate constants ($k_{f2}$, pH 7, 40°C) with [GuHCl] and folding free energy. Open circles, 308-nm excitation; solid circles, 266-nm excitation.

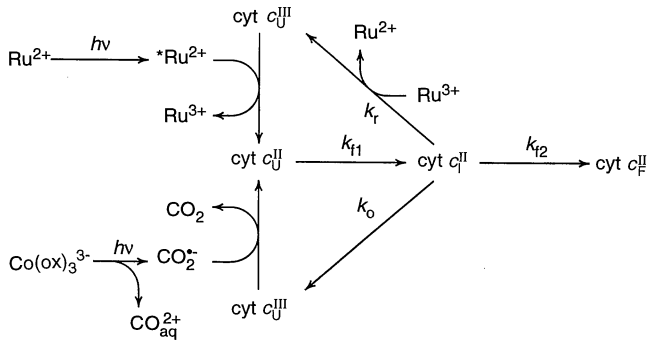


**Fig. 3.** Photochemical methods for injecting electrons into unfolded cyt $c^{II}$. $*Ru^{2+}$ is the electronically excited Ru(2,2′-bipyridine)$_3^{2+}$ ion. Photochemical electron injection from this complex is reversible and can be used in studies of submillisecond protein folding. Irradiation of $Co(ox)_3^{3-}$ is used for studies of protein folding on longer time scales.

$c^{III}$ (*29*). Hence, at a constant driving force, the enthalpy and entropy changes for folding cyt $c^{II}$ are substantially more negative than those for cyt $c^{III}$.

The topography of the energy surface for folding has important kinetic consequences: a rough surface indicates that the protein has many low-energy nonnative configurations separated by high energy barriers (*1*, *30*). Cyt $c^{III}$ folding has been shown to lead to structures with nonnative His ligands bonded to the Fe center (*3–5*, *24*). These incorrectly folded structures rearrange quite slowly to the native structure. We see no corresponding processes in cyt $c^{II}$, perhaps because the ferroheme center does not bind a second His ligand as tightly as does a ferriheme. In other words, there may be deeper traps in the cyt $c^{III}$ folding surface.

The complex process of protein folding involves dynamics on time scales that range from picoseconds to minutes. In the picosecond to nanosecond time regime, it is possible to study the motions of amino acid side chains and the folding or unfolding of short peptide segments (*31*). Until very recently, studies of whole-protein folding have been limited to the millisecond and longer time regime, where molten globules collapse to tightly folded structures (*7*). The nanosecond to millisecond gap in measurement times is believed to encompass secondary structure formation and the collapse to compact denatured structures. Rapid initiation of protein folding by electron transfer should be able to bridge this gap.

## REFERENCES AND NOTES


1. J. N. Onuchic, P. G. Wolynes, Z. Luthey-Schulten, N. D. Socci, *Proc. Natl. Acad. Sci. U.S.A.* **92**, 3626 (1995).
2. M. Karplus and D. L. Weaver, *Protein Sci.* **3**, 650 (1994); A. M. Gutin, V. I. Abkevich, E. I. Shakhnovich, *Proc. Natl. Acad. Sci. U.S.A.* **92**, 1282 (1995).
3. C. M. Jones *et al.*, *Proc. Natl. Acad. Sci. U.S.A.* **90**, 11860 (1993).
4. G. Elöve, A. K. Bhuyan, H. Roder, *Biochemistry* **33**, 6925 (1994).
5. T. R. Sosnick, L. Mayne, R. Hiller, S. W. Englander, *Nature Struct. Biol.* **1**, 149 (1994).
6. R. L. Baldwin, *Bioessays* **16**, 207 (1994); A. R. Fersht, *Curr. Opin. Struct. Biol.* **5**, 79 (1995).
7. O. B. Ptitsyn, *Adv. Protein Chem.* **47**, 83 (1995).
8. S. W. Englander, L. Mayne, *Annu. Rev. Biophys. Biomol. Struct.* **21**, 243 (1992).
9. B. Nötling, R. Golbik, A. R. Fersht, *Proc. Natl. Acad. Sci. U.S.A.* **92**, 10668 (1995). Barstar is the polypeptide inhibitor of *Bacillus amyloliquefaciens* ribonuclease (barnase).
10. J. Bixler, G. Bakker, G. McLendon, *J. Am. Chem. Soc.* **114**, 6938 (1992).
11. R. Santucci, H. Reinhard, M. Brunori, *ibid.* **110**, 8536 (1988).
12. V. T. Taniguchi, N. Sailasuta-Scott, F. C. Anson, H. B. Gray, *Pure Appl. Chem.* **52**, 2275 (1980).
13. These folding curves are also temperature dependent; folding midpoints shift to lower [GuHCl] at higher temperatures.
14. N. Sutin and C. Creutz, in *Inorganic and Organometallic Photochemistry*, M. S. Wrighton, Ed. (American Chemical Society, Washington, DC, 1978), vol. 168, pp. 1–27.
15. In this bimolecular electron-injection scheme, the decay time of $*Ru^{2+}$ defines the short-time limit for protein-folding measurements. The nanosecond time scale can be achieved with intramolecular electron-injection methods.
16. R. M. Ballew, J. Sabelko, M. Gruebele, *Proc. Natl. Acad. Sci. U.S.A.*, in press.
17. The reoxidation rate appears to be independent of [GuHCl].
18. A study of the early events in cyt $c^{II}_U$ folding (initiated by photodissociation of CO) suggests that ferroheme axial-ligand exchange kinetics occur on a submillisecond time scale (*3*).
19. At higher [GuHCl], our measured $k_{f2}$ values appear to level off, but the uncertainties in these rates are quite large because of the competition from $k_o$. There has been one report of cyt $c^{II}$ folding measured with stopped-flow methods (*3*). The observed rate constant ($k_f$ = 1.0 ± 0.1 $s^{-1}$ at 4.6 M GuHCl and 40°C) agrees quite well with the 1.3 $s^{-1}$ estimated from our data.
20. B.-L. Chen, W. A. Baase, H. Nicholson, J. A. Schellman, *Biochemistry* **31**, 1464 (1992).
21. G. McLendon and M. Smith, *J. Biol. Chem.* **253**, 4004 (1978).
22. D. S. Cohen and G. J. Pielak, *J. Am. Chem. Soc.* **117**, 1675 (1995).
23. K. Kuwajima, H. Yamaya, S. Miwa, S. Sugai, T. Nagamura, *FEBS Lett.* **221**, 115 (1987); Y. Bai, T. R. Sosnick, L. Mayne, S. W. Englander, *Science* **269**, 192 (1995).
24. J. Babul and E. Stellwagen, *Biopolymers* **10**, 2359 (1971); *Biochemistry* **11**, 1195 (1972).
25. This value was estimated from the variation of $k_{f2}$ over the 20° to 40°C temperature range.
26. Although this was not the dominant folding phase observed at pH 6.9 (*4*), we believe that the conformational changes associated with this phase are most closely related to those we observed with cyt $c^{II}$.
27. P. Bertrand *et al.*, *Biochemistry* **34**, 11071 (1995).
28. E. L. Yee, R. J. Cave, K. L. Guyer, P. D. Tyma, M. J. Weaver, *J. Am. Chem. Soc.* **101**, 1131 (1979).
29. G. I. Makhatadze and P. L. Privalov, *J. Mol. Biol.* **232**, 639 (1993); P. L. Privalov and G. I. Makhatadze, *ibid.*, p. 660. The folding thermodynamics extracted from electrochemical measurements are at variance with those obtained from studies of thermal denaturation of cyt $c^{II}$ in acidic solutions (*22*).
30. J. D. Bryngelson, J. N. Onuchic, P. G. Wolynes, *Proteins Struct. Funct. Genet.* **21**, 167 (1995).
31. L. X.-Q. Chen, J. W. Petrich, G. R. Fleming, A. Perico, *Chem. Phys. Lett.* **139**, 55 (1987); J. M. Beals, E. Haas, S. Krausz, H. A. Scheraga, *Biochemistry* **30**, 7680 (1991); W. H. Woodruff, R. B. Dyer, R. H. Callender, K. Paige, T. Causgrove, *Biophys. J.* **66**, A397 (1994); C. M. Phillips, Y. Mizutani, R. M. Hochstrasser, *Proc. Natl. Acad. Sci. U.S.A.* **92**, 7292 (1995).


32. We thank G. Mines and S. Lee for technical assistance, M. Gruebele for a preprint of his paper on apomyoglobin, and P. Wolynes for helpful discussions. Supported by the Swedish Natural Science Research Council (T.P.), NIH, NSF, and the Arnold and Mabel Beckman Foundation.

5 December 1995; accepted 29 January 1996


# Microsecond Catalytic Partial Oxidation of Alkanes


Duane A. Goetsch and Lanny D. Schmidt*



A single layer of woven platinum–10 percent rhodium gauze was used as a catalyst for the partial oxidation of ethane, propane, *n*-butane, and isobutane. This configuration produced oxygen conversions of equal to or greater than 90 percent and had high selectivity to olefins and oxygenated hydrocarbons at contact times as short as 10 microseconds at atmospheric pressure. This reactor operates by rapid chemical heating (~5 microseconds) followed by rapid quenching to avoid homogeneous reactions, which decompose products. Mixing of the cold unreacted gas passing between the gauze wires with the hot product gas results in rapid quenching (~200 microseconds) of the products from ~800° to ~400°C. The rapid quenching avoids successive homogeneous decomposition reactions of unstable products such as olefins and aldehydes but still allows homogeneous chain reactions that produce these species. The strong variations in products with the feed alkane showed that the reaction pathways operating at ~$10^{-5}$ seconds are quite different than those operating at longer residence times. These results could have a significant effect on the direct conversion of alkanes to oxygenates such as formaldehyde.


Catalytic partial oxidation processes offer great potential for the fast, efficient, and economical conversion of light alkanes associated with remote sources of natural gas into more valuable liquid fuels and chemicals. A crucial feature of such processes is the ability to attain high surface reaction rates to minimize contributions from nonselective homogeneous reactions to produce $CO_2$ and $H_2O$, thus allowing selective catalytic partial oxidation processes to dominate.


Department of Chemical Engineering and Materials Science, University of Minnesota, Minneapolis, MN 55455, USA.

*To whom correspondence should be addressed.


Different catalytic monolith chemical reactor configurations are sketched in Fig. 1. The catalysts could be either metal-coated ceramic monoliths, transition metal oxide coated onto ceramic monoliths, or metal gauzes. Lower activity catalysts typically require the reactants to be preheated to achieve the desired reaction rate; however, preheating the reactants by conventional heat transport through the reactor walls produces significant homogeneous reaction before the reactants contact the catalyst (Fig. 1A).

Previously, we showed that porous α-alumina monoliths coated with Rh (for syngas) (*1*, *2*) or with Pt (for olefins) (*3*) operate autothermally and give essentially complete